Theory and Implementation of Wireless Transponders

Dai Enguang, *Member, IEEE*

***Abstract*—A theoretical analysis for the surface-acoustic-wave-based wireless transponder in a wireless system has been proposed in this paper. Radio transponders were also implemented based upon the theory of coupling of modes. The proposed theory can be employed in the simulation of amplitude- and phase-coded devices with different segments.**

***Index Terms*—SAW, telemetry, transponders.**

I. Introduction

It has long been known that the surface acoustic wave (SAW) transponder is suitable for mainly two applications: passive identification and passive sensing [1]–[4]. The schematic layout of the transponders is that the SAW transducer connected to a receiving antenna receives an electromagnetic wave burst emitted from the interrogation unit. The SAW is then excited and transported along the piezoelectric crystal. When the SAW is intercepted by coded reflectors and reflects parts of the incoming wave, these echoes will be transported back into an electromagnetic signal at the same transducer. Using an on/off keying with 16 reflectors, 2^{16} objects can be identified. However, for sensing purposes, fewer reflectors are enough. Unlike identification systems, the echo impulse in sensing systems is evaluated by its phase with the transmitted signal rather than by its amplitude, in which the phase shift can be calculated from two components with high resolution.

There are many kinds of structures that can be employed in the implementation of coded transponders. The staggered structure shown in Fig. 1(a), the in-line architectures shown in Fig. 1(b) and (c) are commonly adopted. The barcode device is, in general, different from that of a phase encoder with one segment. However, if each phase-coded reflector is separated in space, the basic theory model will be similar for both the amplitude and phase encoders with distributed and separated reflectors. Although transponders have been fabricated in some laboratories, there has yet to be a theory reported for the design of transponders. In this paper, taking the in-line structure with reflectors on one side of the transducer as an example, the author will establish the theory for the design of wireless transponders.

II. Theory and Implementation

SAW-based wireless and passive transponders are commonly pulse operated. A versatile coupling-of-mode (COM) approach can also be employed for the analysis of the overall transponder. Fig. 2 represents the corresponding building blocks of the transponder shown in Fig. 1(c) with three reflectors. T_1 denotes the transducer, while T_{out} is its image transducer located at the place of the real transducer. It is not a real transducer; it is only a model for the analysis of the transponder. In these building blocks, $[G_3]$, $[G_5]$, and $[G_7]$ are 2×2 transmission matrices of the three reflectors, respectively. $[D_2]$, $[D_4]$, and $[D_6]$ are acoustic transmission-line matrices in which $[D_2]$ is the transmission matrix between the first reflector and transducer, while $[D_4]$ and $[D_6]$ denote the transmission matrixes between the first and second reflectors and the second and last reflectors, respectively.

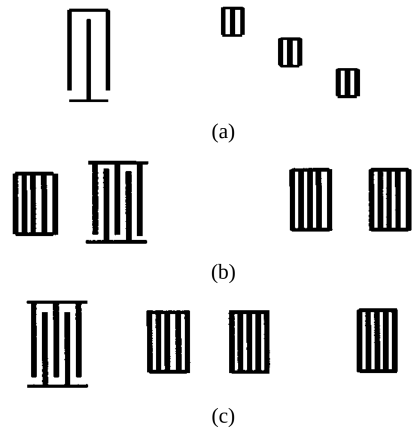

Fig. 1. (a) Transponder of a staggered structure. (b) Transponder of an in-line structure with reflectors on both sides of the transducer. (c) Transponder of an in-line structure with reflectors on one side of the transducer.

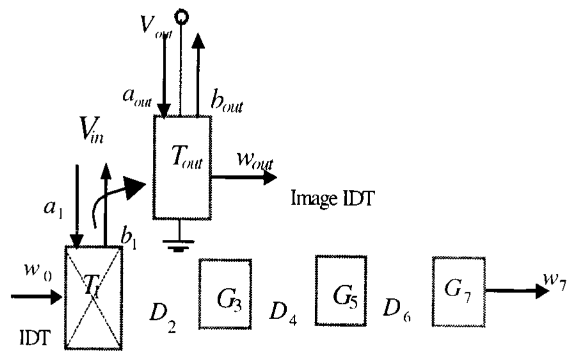

Fig. 2. SAW transponders in terms of its building blocks.

If we denote the amplitude of the forward- and the backward-going SAW by w^+ and w^-, the COM equation can be expressed as

$$\frac{dw^+(x)}{dx} = -jk_{11}w^+(x) + jk_{12}w^-(x) + j\alpha V \tag{1}$$

$$\frac{dw^-(x)}{dx} = -jk_{11}w^-(x) - jk_{12}^*w^-(x) - j\alpha^* V \tag{2}$$

$$\frac{dI}{dx} = -2j\alpha^* w^+(x) + 2j\alpha w^-(x) + j\omega CV \tag{3}$$

Manuscript received October 22, 2000; revised January 14, 2001.

The author is with National Laboratory on Local Fiber-Optic Communication Networks and Advanced Optical Communication Systems, Department of Electronics, Peking University, 100871 Beijing, China.

Publisher Item Identifier S 0018-9480(01)02909-X.

where k_{11} is the self-coupling coefficient and k_{12} is the mode coupling coefficient, respectively, C is the capacitance per unit length, V is the voltage, $I(x)$ denotes the busbar current, and α is the transduction coefficients. Based upon the differential equations, both the matrix $[T]$ of the interdigital transducer (IDT) and the grating matrix $[G]$ can be determined [5]–[7] as follows:

$$\begin{pmatrix} w_{i-1}^{+} \\ w_{i-1}^{-} \\ b_i \end{pmatrix} = [T] \begin{pmatrix} w_i^{+} \\ w_i^{-} \\ a_i \end{pmatrix}. \tag{4}$$

The elements of the matrix $[T]$ are given by

$$[T] = \begin{bmatrix} t_{11} & t_{12} & t_{13} \\ -t_{12} & t_{22} & t_{23} \\ st_{13} & -st_{23} & t_{33} \end{bmatrix}.$$

Assuming that the finger reflection effects can be neglected

$$[T] = \begin{bmatrix} s(1+t_0)e^{j\theta_t} & -st_0 & t_{13} \\ st_0 & s(1-t_0)e^{-j\theta_t} & t_{13}e^{-j\theta_t} \\ st_{13} & -st_{13}e^{-j\theta_t} & t_{33} \end{bmatrix}$$

where f_0 is the center frequency, the symmetry parameter for the IDT with N_i electrodes $s = (-1)^{N_i}$

$$t_0 = G_a(R_s + Z_e)/(1 + j\theta_e).$$

Here, R_s is the metal resistance of the transducer.

Radiation conductance are obtained as [5]

$$G_a = 8K^2 C_s f_0 (N_t - 1)^2 \left[\sin\left(\frac{\theta_t}{2}\right) \Big/ \left(\frac{\theta_t}{2}\right) \right]^2.$$

The radiation susceptance is

$$B_a = 16K^2 C_s f_0 (N_t - 1)^2 \left[\frac{\sin(\theta_t) - \theta_t}{\theta_t^2} \right]$$
$$t_{13} = \frac{\sqrt{2G_a Z_e}}{1 + j\theta_e} e^{j\theta_t/2}.$$

Here, Z_e is load resistance

$$t_{33} = 1 - \frac{2j\theta_c}{1 + j\theta_e}$$

where

$$\theta_t = N_t \lambda \delta_t / 2$$
$$\theta_c = \omega C_T (R_s + Z_e)$$

and

$$\theta_e = (\omega C_T + B_a)(R_s + Z_e)$$

where C_s is static capacitance per electrode pair, C_T is the total IDT capacitance, and K^2 is the electromechanical coupling constant. The detuning parameter in the region of the transducer can be expressed as

$$\delta_t = \frac{2\pi(f - f_0)}{v_t}$$

where v_t is the phase velocity in the transducer.

The acoustic submatrix is

$$[t_i] = \begin{bmatrix} t_{11} & t_{12} \\ -t_{12} & t_{22} \end{bmatrix}_i.$$

The electrical signal b_i leaving the IDT is given by

$$b_i = [\tau_i'][W_i] + a_i \cdot (t_{33})_i \tag{5}$$

where

$$[\tau_i] = \begin{bmatrix} t_{13} \\ -t_{23} \end{bmatrix}_i \quad \text{and} \quad [\tau_i'] = s \cdot \begin{bmatrix} t_{13} \\ -t_{23} \end{bmatrix}_i.$$

As far as the reflector is concerned, the reflection effects between strips are included in the model. The scattering matrix $[S]$ presents the solutions to the COM equations

$$\begin{pmatrix} w_{i-1}^{-} \\ w_i^{+} \end{pmatrix} = [S] \begin{pmatrix} w_{i-1}^{+} \\ w_i^{-} \end{pmatrix}.$$

The solution for the reflector can be derived from (1)–(3).

The detuning complex parameter in the region of reflectors is obtained as

$$\delta_r = \frac{\omega - \omega_0}{v_g} - j\gamma.$$

Here, v_g is the SAW phase velocity in the grating and γ is the attenuation coefficient. Considering the reflectivity coupling, the detuned version of δ_r is

$$D = \sqrt{\delta_r^2 - R^2}.$$

R is the reflectivity coefficient from one electrode and L denotes the length of the reflector. The elements of the scattering matrix are

$$S_{11} = \left. \frac{w^{-}(0)}{w^{+}(0)} \right|_{w^{-}(L)=0} = \frac{jR\sin(DL)}{D\cos(DL) + j\Delta\sin(DL)}$$
$$S_{12} = \left. \frac{w^{-}(0)}{w^{-}(L)} \right|_{w^{+}(0)=0} = \frac{D}{D\cos(DL) + j\Delta\sin(DL)} \exp(-jk_0 L)$$

where $k_0 = \omega / v_g$ is a wavenumber of SAW propagation and ω is the radian frequency of the wave. Using the reciprocity for the matrix, the remaining formulas are found as follows:

$$S_{21} = S_{12} \quad S_{22} = S_{11}.$$

The forward and backward SAW w_{i-1}^{+}, w_{i-1}^{-} are associated with the ith reflector. The transmission equation is given as

$$\begin{pmatrix} w_{i-1}^{+} \\ w_{i-1}^{-} \end{pmatrix} = [G] \begin{pmatrix} w_i^{+} \\ w_i^{-} \end{pmatrix}.$$

The transmission matrix

$$[G] = \begin{pmatrix} G_{11} & G_{12} \\ G_{32} & G_{22} \end{pmatrix}.$$

The elements of the transmission matrix are

$$G_{11} = \frac{D\cos(DL) + j\Delta\sin(DL)}{D}.$$

In addition

$$G_{12} = -\frac{jR\sin(DL)}{D}, \quad G_{21} = \frac{jR\sin(DL)}{D}$$

and

$$G_{22} = \frac{D^2\exp^2(-jk_0L) + R^2\sin^2(DL)}{D(D\cos(DL) + j\Delta\sin(DL))}.$$

The equation for acoustic waves at the $(i-1)$th and ith reference planes is

$$[W_{i-1}] = [t_i][W_i] + a_i \cdot [\tau_i] \tag{6}$$

where a_i is the input electrical signal at the ith plane and $[t_i]$ is the acoustic submatrix.

From (6), the transmission equation associated with the transducer is given by

$$[W_0] = [t_1][W_1] + a_1\tau_1. \tag{7}$$

The acoustic wave transmission can be described as

$$[W_1] = [D_2][G_3][D_4][G_5][D_6][G_7][W_7]. \tag{8}$$

where the transmission-line matrix $[D]$ is

$$[D_i] = \begin{bmatrix} e^{j\beta L_i} & 0 \\ 0 & e^{-j\beta L_i} \end{bmatrix}$$

$\beta = 2\pi/\lambda$, L_i is the acoustic transmission-line length of the ith reflector between appropriate reference planes. The overall acoustic matrix $[M]$ is now obtained as the product of the composite building blocks

$$[M] = [t_1][D_2][G_3][D_4][G_5][D_6][G_7] \tag{9}$$

$$[W_0] = [t_1][D_2][G_3][D_4][G_5][D_6][G_7][W_7] + a_1[\tau_1]$$

$$\begin{pmatrix} w_0^+ \\ w_0^- \end{pmatrix} = [M]\begin{pmatrix} w_7^+ \\ w_7^- \end{pmatrix} + a_1[\tau_1]. \tag{10}$$

As there is no SAW externally incident on the transducer and gratings, set

$$w_0^+ = w_7^- = 0. \tag{11}$$

The output of the transducer is given by

$$[W_{\rm out}] = [D_2][G_3][D_4][G_5][D_6][G_7][W_7]$$

$$[\tau_1'] = s \cdot \begin{pmatrix} t_{13} \\ -t_{23} \end{pmatrix}_1. \tag{12}$$

The electrical output voltage is

$$V_{\rm out} = b_{\rm out} = [\tau_1'] \cdot [W_{\rm out}] \tag{13}$$

and the phase response is

$$\Phi(f) = \tan^{-1}\left\{\frac{\text{Imaginary}(V_{\rm out})}{\text{Real}(V_{\rm out})}\right\} \tag{14}$$

$$b_1 = a_{\rm out} = 0. \tag{15}$$

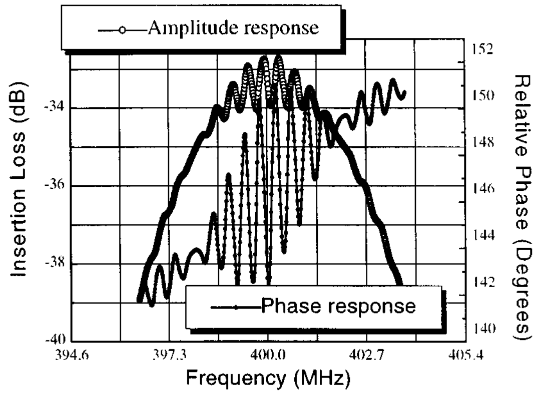

Fig. 3. Calculated frequency response of the transponder.

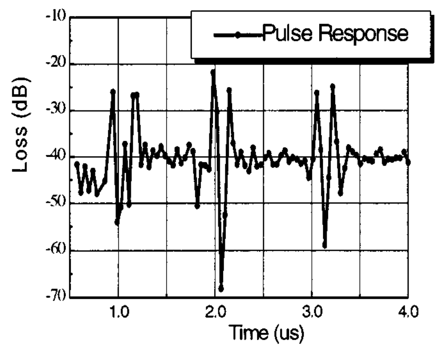

Fig. 4. Calculated impulse response of the transponder.

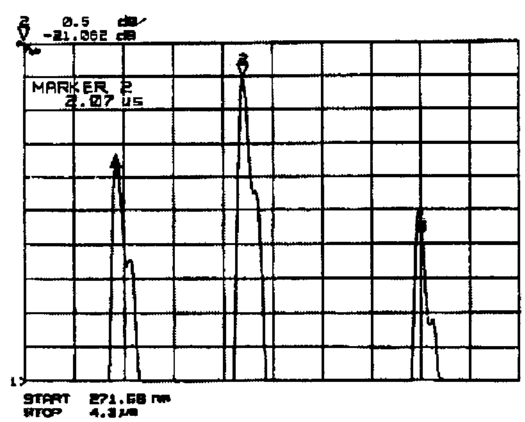

Fig. 5. Experimental impulse response.

In the simulation of the 400-MHz $yz - LiNbO_3$-based transponders with three reflectors, source and load resistance were 50 Ω and the finger pairs of the transducer was 20. From (13) and (14), the amplitude and phase response can be calculated. Fig. 3 shows the theoretical frequency response of the transponder. Based upon the predicted amplitude response and phase response, an inverse fast Fourier transform (FFT) was employed to calculate the theory impulse response shown in Fig. 4. In this figure, three envelopes of the burst pulse denote three real pulses. It should be noted that when implementing a practical transponder, impedance matching and optimum reflective efficiency should be considered. The experimental response of the transponder is depicted in Fig. 5. The comparison between experimental and predicted pulse

TABLE I
EXPERIMENTAL AND PREDICTED PULSE ECHO DELAY (UNIT: microseconds)

Echo	Calculation	Experiment
The First pulse position	1.1	1.03
The Second pulse position	2.1	2.07
The Third Pulse position	3.25	3.5

echo delay is listed in Table I. The minimum relative error is 1.4%, corresponding to the second pulse, the maximum error is 7%, coming from the last echo, which resulted mainly from the fabrication errors and SAW velocity discrepancy between the calculation and experiment. Though the echo delay for the three pulses can be simply determined, this consistence can prove the validity of the model. The relative amplitude of the impulse response of these reflectors can be figured out by Fig. 4. If more sample points were used, the pulsewidth can be determined by this figure. In fact, for the calculation of the time position of the reflective pulses, we do not need any new theory. It can be calculated very quickly merely based upon SAW velocity and the distance between the transducer and reflectors. In this paper, the time position calculation can prove the effectiveness of the overall modeling. To predict the absolute reflection loss of the device accurately, we need loss and attenuation related accurate parameters such as the grating loss coefficient, grating mutual coupling coefficient, and other factors, including the matching and fabrication conditions. In most circumstances, these parameters that relate with a concrete device were not accurate enough to precisely predict the absolute echo loss. Thus, the reflective loss comparison between theory and experiment is not made in this paper. If accurate COM parameters are available, based upon the approach developed here, precise prediction of reflective loss can be realized.

In [4], a special single-phase unidirectional transducer (SPUDT) with different ring-to-rung periodicity was designed. An electrode width-controlled SPUDT is rarely employed in SAW transponders for its $\lambda/8$ finger width. If the passive sensing technology combines with sensor array technology, a more sophisticated multitag array capable of discrimination between different parameters can be built [8].

It should to be noted that the image IDT concept, separating the transducer in an in- and out-coupling transducer, is not absolutely necessary for the modeling of the overall transponder. The device can be calculated as it is, i.e., a one-port device. We can take the standard SAW calculation method for the SAW transponders, calculate S_{11}, and apply a Fourier transformation. However, as far as this reflective one-port device is concerned, it is more convenient to establish a cascaded matrix for the overall device. Since the single transducer does function as the coupling in driving signal and coupling out reflective impulses, introducing the concept of image IDT into the theory will be helpful for the modeling of one-port SAW device, especially the one-port transponder.

III. CONCLUSIONS

The theory for the implementation of SAW-based wireless transponders has been established. The proposed theory can be employed in the simulation of distributed amplitude- and phase-coded devices with different segments. The basic model of the theory can be further evolved. If second-order effects such as bulk wave interference, electromagnetic feedthrough, diffraction, etc. are included in the COM-based model, a more precise prediction can be achieved. The author only established the theory model; other factors can be embedded into the frame according to different calculation precision or system requirements.

REFERENCES

[1] A. Pohl, "A low-cost high-definition wireless sensor system utilizing intersymbol interference," *IEEE Trans. Ultrason., Ferroelect., Freq. Contr.*, vol. 45, pp. 1355–1362, Sept. 1998.

[2] L. Reindl, G. Scholl, T. Ostertag, H. Scherr, U. Wolff, and F. Schmidt, "Theory and application of passive SAW radio transponders as sensors," *IEEE Trans. Ultrason., Freq. Contr.*, vol. 45, pp. 1281–1292, Sept. 1998.

[3] D. Enguang and F. Guangping, "The passive sensors based upon SAW ID-tags," in *Proc. Asia–Pacific Microwave Conf.*, vol. 2, India, 1996, pp. 703–707.

[4] D. Enguang, "Passive and remote sensing based upon SAW in special environments," in *IEEE Microwave Optoelectron. Conf.*, Natal, Brazil, 1997, pp. 133–139.

[5] C. Campbell, *Surface Acoustic Wave Devices and Their Signal Processing Applications*. New York: Academic, 1989.

[6] D. P. Chen and H. A. Haus, "Analysis of metal strip SAW gratings and transducers," *IEEE Trans. Ultrason., Ferroelect., Freq. Contr.*, vol. UFFC-42, pp. 395–408, May 1985.

[7] B. P. Abbott *et al.*, "A coupling-of-modes analysis of chirped transducers containing reflective electrode geometries," in *IEEE Ultras. Symp. Dig.*, 1989, pp. 129–134.

[8] D. Enguang, "State-of-the-art instruments based upon SAW wireless tags, SAW match filters, and SAW resonators," in *IEEE Ultrason. Symp. Dig.*, vol. 1, 1999, pp. 425–428.

Dai Enguang (M'00) received the Ph.D. degree from Tsinghua University, Beijing, China, in 1997.

From 1997 to 1999, he was a Post-Doctoral Fellow in the Department of Electronics, Peking University, Beijing, China. He is currently an Associate Professor in the Department of Electronics, Peking University. His research interests are in the fields of optical-fiber communication, SAW devices, integrated optics devices, microwaves, microelectromechanical systems (MEMS), sensor arrays, and low-noise oscillator and spread-spectrum technologies.